

Supplementary Information

Reactivity of Atomically Dispersed Pt²⁺ Species towards H₂: Model Pt–CeO₂ Fuel Cell Catalyst

Yaroslava Lykhach,^{a*} Alberto Figueroba,^b Matteo Farnesi Camellone,^c Armin Neitzel,^a Tomáš Skála,^d Fabio R. Negreiros,^c Mykhailo Vorokhta,^d Nataliya Tsud,^d Kevin C. Prince,^{e,f} Stefano Fabris,^c Konstantin M. Neyman,^{b,g} Vladimír Matolín,^d Jörg Libuda^{a,h}

^aLehrstuhl für Physikalische Chemie II, Friedrich-Alexander-Universität Erlangen-Nürnberg,
Egerlandstrasse 3, 91058 Erlangen, Germany

^bDepartament de Química Física and Institut de Química Teòrica i Computacional (IQTCUB),
Universitat de Barcelona, c/ Martí Franquès 1, 08028 Barcelona, Spain

^cCNR-IOM DEMOCRITOS, Istituto Officina dei Materiali, Consiglio Nazionale delle Ricerche
and SISSA, Via Bonomea 265, I-34136, Trieste, Italy

^dCharles University, Faculty of Mathematics and Physics, Department of Surface and Plasma
Science, V Holešovičkách 2, 18000 Prague, Czech Republic

^eElettra-Sincrotrone Trieste SCpA, Strada Statale 14, km 163.5, 34149 Basovizza-Trieste, Italy
^fIOM, Strada Statale 14, km 163.5, 34149 Basovizza-Trieste, Italy

^gInstitució Catalana de Recerca i Estudis Avançats (ICREA), 08010 Barcelona, Spain

^hErlangen Catalysis Resource Center, Friedrich-Alexander-Universität Erlangen-Nürnberg,
Egerlandstrasse 3, 91058 Erlangen, Germany

1. Destabilizing effect of oxygen vacancies on the adsorption energy of Pt²⁺

1.1. The role of the vacancy location and the distribution of Ce³⁺ ions

We studied the influence of the location of oxygen vacancies O_{vac} on the adsorption energy of Pt²⁺. First, the square oxygen nanopocket site O₄ has been considered on Ce₄₀O₈₀ NP for interaction with one Pt atom (Figure S1). The oxygen vacancies have been created in the positions +10, +5, +2 at the decreasing distance from the Pt²⁺ site. The corresponding adsorption energies of Pt²⁺ are summarized in the Table S1 as a function of the distribution of Ce³⁺ cations around the vacancy. We found that the adsorption energy decreases in magnitude with decreasing distance from O_{vac} to the Pt²⁺ site.

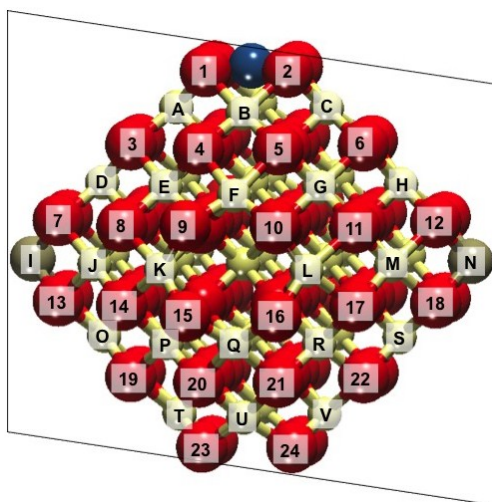


Figure S1. Pt–Ce₄₀O₈₀ model. The transparent plane cuts the nanoparticle into two symmetric halves. The positions of O vacancies and Ce³⁺ ions are labeled by the numbers and the capital letters, respectively.

With respect to the experimental cohesive energy of the bulk Pt (-5.85 eV),^{S1} the formation of the oxygen vacancies in the positions +10 and +5 do not have a significant impact on stability of Pt²⁺. Only when an O_{vac} is created inside the O₄ nanopocket (position +2) the adsorbed atomic Pt is calculated to be less stable than in the Pt bulk ($E_{ad} = -4.99$ eV). However, the energy of the vacancy formation in the position +2 is by 1.2 and 0.6 eV higher in comparison to these calculated for the positions +10 and +5, respectively. Since the energy value of the vacancy formation is decreasing with increasing distance from the Pt²⁺ site, we assume that the oxygen vacancies will be first formed far from the Pt²⁺ site and they will not have a significant impact on the stability of Pt²⁺.

1.2. The threshold concentration of oxygen vacancies and the role of the Pt²⁺

In the next step we investigated the stability of Pt²⁺ as a function of O_{vac} concentration. We employed the 4Pt–Ce₄₀O₈₀ model that accommodated four Pt²⁺ sites (Figure S2). The obtained results are summarized in Table S2. We found that formation of one O_{vac} per each Pt²⁺ site exhibits a similar trend with respect to the distance from the Pt²⁺ site as on the Pt–Ce₄₀O₈₀ models. However, formation of four oxygen vacancies in the positions (4, 21, -5, -20) in

4Pt–Ce₄₀O₈₀ model (equivalent to a single O_{vac} in +5 position of Pt–Ce₄₀O₈₀ model) has larger effect on the stability of Pt²⁺ from 0.4 eV to 0.8 eV. This suggests that reduction of Pt²⁺ is more facile at higher Pt concentration in Pt–CeO₂ films.

Table S1. Adsorption energies of Pt²⁺ (E_{ad}) and the energies of oxygen vacancy O_{vac} formation (E_{vac}) on Pt–Ce₄₀O_{80-n} model. The O vacancy positions with the signs “+” and “-” are in front of and behind the plane (see Figure S1), respectively.

Pt state	O _{vac} positions	Ce ³⁺ positions	E_{ad} , eV	E_{vac} , eV
Pt ²⁺		I, N	-7.02	–
Pt ²⁺	+10	F, I, L, N	-6.24	1.57
Pt ²⁺	+5	E, H, I, N	-6.60	2.24
Pt ²⁺	+5	D, G, I, N	-6.59	2.25
Pt ²⁺	+5	E, G, H, I	-6.55	2.29
Pt ²⁺	+5	H, I, J, N	-6.51	2.33
Pt ²⁺	+5	D, E, I, N	-6.48	2.37
Pt ²⁺	+5	G, H, I, N	-6.47	2.38
Pt ²⁺	+5	G, I, J, N	-6.47	2.37
Pt ²⁺	+5	E, I, M, N	-6.47	2.37
Pt ²⁺	+5	G, I, M, N	-6.32	2.53
Pt ²⁺	+5	D, I, J, N	-6.30	2.54
Pt ²⁺	+5	A, C, E, N	-6.24	2.61
Pt ²⁺	+2	A, C, I, N	-4.99	2.83
Pt ¹⁺	+2	D, H, N	-4.63	3.19
Pt ¹⁺	+2	D, I, N	-4.62	3.19
Pt ¹⁺	+2	D, H, -M	-4.55	3.27
Pt ²⁺	±2	A, ±B, C, I, N	-5.38	2.14
Pt ²⁺	+2, -1	A, ±B, C, I, N	-4.75	2.14

As discussed in the main text of the manuscript, formation of eight O vacancies per four Pt²⁺ sites (two O_{vac} per one Pt²⁺ site) far from the O₄ nanopocket leads to a significant decrease of Pt²⁺ adsorption energy value. This suggests that the threshold concentration of oxygen vacancies with respect to Pt²⁺ around 2:1 should be reached before the onset of Pt²⁺ reduction.

Table S2. Adsorption energies of Pt²⁺ (E_{ad}) and the energies of oxygen vacancy O_{vac} formation (E_{vac}) on 4Pt–Ce₄₀O_{80-n} model. The O vacancy positions with the signs “+” and “-” are in front of and behind the plane (see Figure S2), respectively.

Pt state	O_{vac} positions	Ce ³⁺ positions	E_{ad} , eV	E_{vac} , eV
4 Pt ²⁺		-B, H, I, -J, K, N, -P, T	-6.59	–
1 Pt ¹⁺ , 3 Pt ²⁺	+2	D, G, H, ±J, ±M, O, S	-6.10 (-4.55*/-6.62)**	2.97
1 Pt ¹⁺ , 3 Pt ²⁺	+2	D, H, ±J, ±M, O, R, S	-6.06 (-4.39*/-6.62)**	3.13
1 Pt ¹⁺ , 3 Pt ²⁺	+2	E, I, ±K, ±M, N, O, S	-5.99 (-4.12*/-6.62)**	3.40
4 Pt ²⁺	+5	D, E, G, H, ±J, ±M, O, S	-6.30	2.18
1 Pt ⁰ , 3 Pt ²⁺	±2	A, C, D, H, ±J, ±M, O, S	-6.14 (-4.78*/-6.59)**	2.33
1 Pt ⁰ , 3 Pt ²⁺	±2	C, D, F', H, ±J, ±M, O, S	-6.05 (-4.45*/-6.59)**	2.49
1 Pt ⁰ , 3 Pt ²⁺	2, -1	D, -E, G, H, ±J, ±M, O, S	-6.22 (-5.25*/-6.54)**	2.16
1 Pt ⁰ , 3 Pt ²⁺	2, -1	D, H, I, ±J, ±M, N, O, S	-6.00 (-4.37*/-6.54)**	2.61
4 Pt ²⁺	6, 19, -3, -22	-B, C, D, G, H, I, -J, K, N, O, ±P, -R, S, T, V	-6.02	2.95
4 Pt ²⁺	4, 21, -5, -20	±B, -E, -F, G, H, I, -J, K, N, - P, ±Q, -R, T, U	-5.77	2.97
3 Pt ⁰ , 1 Pt ¹⁺	2, 15, -16, -23	-F, G, H, I, J, -M, O, -P, S	-5.34	3.02
4 Pt ²⁺	±4, ±5, ±20, ±21	±B, C, ±E, ±F, G, H, I, -J, K, -L, N, ±P, ±Q, Q'±R, T, ±U	-4.57	3.40
4 Pt ²⁺	±3, ±6, ±19, ±22	A, -B, C, D, E, ±G, H, I, ±J, K, ±M, N, O, ±P, ±R, S, T, - U, V	-4.56	3.41

* E_{ad} for the Pt atom near the O_{vac} . ** E_{ad} average for the 3 Pt atoms distant from the O_{vac} . The positions of Ce³⁺ ions labeled F' and Q' are located between the +F and -F and between +Q and -Q, respectively.

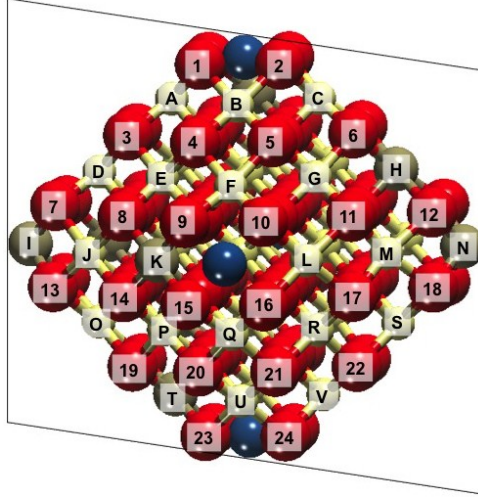


Figure S2. 4Pt–Ce₄₀O₈₀ model. The transparent plane cuts the nanoparticle into two symmetric halves. The O vacancies and the positions of Ce³⁺ ions are labeled by the numbers and the capital letters, respectively.

2. Experimental estimation of the threshold concentration ratio between the number of oxygen vacancies and Pt²⁺ ions.

Upon reverse spillover of oxygen from Pt–CeO₂ substrate onto Pt particle followed by the clean-off reaction with H₂, two Ce³⁺ ions are formed per one oxygen vacancy:



where O_(Pt) is the spilt-over oxygen atom onto Pt particle.

Therefore the density of oxygen vacancies corresponds to one half of the increase in Ce³⁺ concentration upon annealing. Here, we assume that the initial concentration of Ce³⁺ observed at low reaction temperature originates mainly from charge transfer from metallic Pt particles^{S2} and from the redox reaction between Pt and Ce⁴⁺ during the growth of Pt–CeO₂ mixed oxide^{S3} and not from the presence of oxygen vacancies. In addition we have to take into account the fact that upon reduction of one Pt²⁺ two Ce³⁺ centers are oxidized to Ce⁴⁺:



These Ce⁴⁺ centers may again be reduced by formation of oxygen vacancies according to equation (1).

As a result we can estimate the number of oxygen vacancies N_{vac} as:

$$N_{\text{vac}} = \frac{1}{2}\Delta N(\text{Ce}^{3+}) + \Delta N(\text{Pt}^{2+}) \quad (3)$$

where $\Delta N(\text{Ce}^{3+})$ is the increase in the concentration of Ce^{3+} sites upon annealing and $\Delta N(\text{Pt}^{2+})$ is the corresponding loss in the Pt^{2+} concentration (the number of Pt^{2+} reduced to Pt^0). The corresponding calculations are summarized in Table S3.

In order to estimate the threshold ratio between the number of oxygen vacancies and the number of reduced Pt^{2+} species we consider two scenarios: (i) non-homogeneous and (ii) homogeneous distribution of oxygen vacancies on the surface of Pt– CeO_2 .

In case of non-homogeneous distribution (i) oxygen vacancies will initially form along the perimeter of Pt particles. Upon annealing to higher temperatures, the reduced area will expand radially around the Pt particles. The corresponding situation is schematically depicted in the Figure S3.

We assume that all Pt^{2+} species inside the reduced areas (Figure S3, light grey) will be reduced once the threshold concentration of oxygen vacancies is reached. Thus, the threshold ratio between the number of oxygen vacancies and the number of reduced Pt^{2+} can be calculated as $N_{\text{vac}}/\Delta N(\text{Pt}^{2+})$ (see Table S3, green). We note that near the onset of Pt^{2+} reduction (450-500 K), the value of 1.5 is obtained which is in a good agreement with theoretically predicted value of 2.

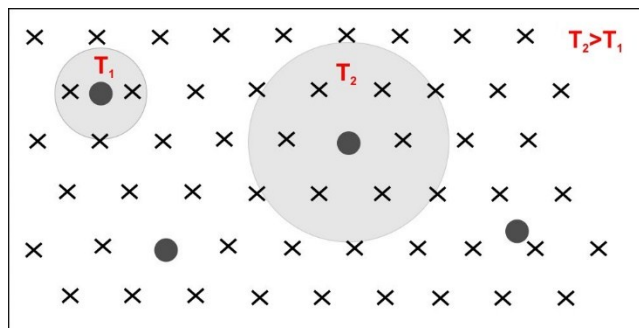


Figure S3. Schematic representation of non-homogeneous distribution of oxygen vacancies (light gray areas) around metallic Pt particles (black circles) at two different temperatures. Pt^{2+} ions are represented by black crosses.

It must be noted that $N_{\text{vac}}/\Delta N(\text{Pt}^{2+})$ ratio could be overestimated if the reduction yields a number of oxygen vacancies above the threshold or if the density of oxygen vacancies in the reduced areas (light gray, Figure S3) has a pronounced gradient with respect to the distance from the Pt particle.

In case of a homogeneous distribution (ii), oxygen vacancies will distribute uniformly across the whole surface. Once the threshold concentration of oxygen vacancies is reached, all Pt^{2+} ions will be reduced instantaneously in a step-like fashion. The region of the steepest decrease of Pt^{2+} signal on 15% Pt– CeO_2 occurs at 550 K (Figure 2b). This means that the threshold concentration of oxygen vacancies is reached at this temperature. The threshold ratio can be calculated at this point as a ratio of the total number of Pt^{2+} present in the film before reduction (350 K, see Table S3) and the number of oxygen vacancies at 550 K. Our calculations yielded value of 0.8. It must be noted, however, that this number is most likely underestimated as a result of not fully uniform distribution of oxygen vacancies at the surface.

Table S3. Experimental estimation of the threshold ratio between the number of oxygen vacancies and Pt^{2+} ions as a function of the reaction temperature.^a

T, K	RER	$\text{Ce}^{3+}/\text{Ce}^{4+}$	$n(\text{Ce}^{3+}) \times 10^{18}$	Pt^{2+}	Pt^0	Pt^*	$N(\text{Pt}^{2+}) \times 10^{18}$	$\Delta N(\text{Pt}^{2+}) \times 10^{18}$	$\Delta N(\text{Ce}^{3+}) \times 10^{17}$	$N_{\text{vac}} \times 10^{18}$	$N_{\text{vac}}/\Delta N(\text{Pt}^{2+})$
110	0.32	0.0576	0.392	13874.0	1889.2	1054.0					
110	0.30	0.0539	0.368	14019.3	832.7	1508.5					
150	0.29	0.0522	0.357	14524.8	343.8	1187.2					
200	0.30	0.0545	0.372	14595.2	248.9	1000.0					
250	0.24	0.0431	0.297	14700.4	390.8	1355.1					
300	0.23	0.0415	0.287	14942.8	398.1	1089.2					
350	0.23	0.0420	0.290	15073.1	432.4	1397.4	2.728	0	0	0	
400	0.23	0.0412	0.285	14684.3	672.9	1238.4	2.658	0.007	-0.051	0.068	0.96
450	0.27	0.0492	0.338	14710.4	1217.1	1178.7	2.662	0.007	0.477	0.090	1.36
500	0.47	0.0848	0.563	13633.9	2310.6	1007.0	2.468	0.026	2.726	0.397	1.52
550	0.92	0.1665	1.028	4474.9	9422.7	1359.2	0.810	1.918	7.375	2.287	1.19
600	1.02	0.1850	1.124	1264.6	11749.8	1007.7	0.229	2.499	8.340	2.916	1.17
650	1.13	0.2052	1.226	870.8	10334.3	950.7	0.158	2.570	9.358	3.038	1.18
700	1.2	0.2183	1.290	581.4	10085.8	613.4	0.105	2.623	9.998	3.122	1.19

^a Pt^{2+} , Pt^0 , and Pt^* designate the integrated intensities of the corresponding components in Pt 4f spectra.

All values in the equations above were calculated from the RPES and SRPES data. First we calculate the concentrations of Ce^{3+} , $N(\text{Ce}^{3+})$, and Pt^{2+} ions $N(\text{Pt}^{2+})$, taking into account the total number of Ce ions in the first monolayer of $\text{CeO}_2(111)$ film ($7.2 \times 10^{18} \text{ m}^{-2}$) and Pt density

($6.62 \times 10^{28} \text{ m}^{-3}$). The calculated values for the 15% Pt–CeO₂ film are shown in Table S3. The Ce³⁺/Ce⁴⁺ was calculated from RER using the calibration.^{S4} The calculations were referenced to the initial concentrations of Ce³⁺ and Pt²⁺ ions at 350 K where no reduction due to formation of vacancies or presence of other adsorbates is observed (highlighted green, Table S3).

3. Supplementary References

- S1. C. Kittel, *Introduction to Solid State Physics, 8th edition*, Wiley 2004.
- S2. G. N. Vayssilov, Y. Lykhach, A. Migani, T. Staudt, G. P. Petrova, N. Tsud, T. Skála, A. Bruix, F. Illas, K. C. Prince, V. Matolín, K. M. Neyman and J. Libuda, *Nat. Mater.*, 2011, **10**, 310-315.
- S3. A. Bruix, Y. Lykhach, I. Matolínová, A. Neitzel, T. Skála, N. Tsud, M. Vorokhta, V. Stetsovych, K. Ševčíková, J. Mysliveček, R. Fiala, M. Václavů, K. C. Prince, S. Bruyere, V. Potin, F. Illas, V. Matolín, J. Libuda and K. M. Neyman, *Angew. Chem., Int. Ed.*, 2014, **53**, 10525–10530.
- S4. T. Staudt, Y. Lykhach, N. Tsud, T. Skála, K. C. Prince, V. Matolín and J. Libuda, *J. Catal.*, 2010, **275**, 181.